

See discussions, stats, and author profiles for this publication at: <https://www.researchgate.net/publication/263940169>

# Salt-concentration dependence of the glass transition temperature in PEO-NaI and PEO-LiTFSI polymer electrolytes

ARTICLE *in* MACROMOLECULES · OCTOBER 2013

Impact Factor: 5.8 · DOI: 10.1021/ma401686r

---

CITATIONS

10

---

READS

64

6 AUTHORS, INCLUDING:



Nicolaas A Stolwijk

University of Münster

139 PUBLICATIONS 2,025 CITATIONS

SEE PROFILE

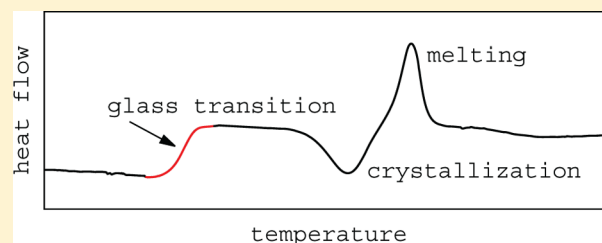
## Salt-Concentration Dependence of the Glass Transition Temperature in PEO–NaI and PEO–LiTFSI Polymer Electrolytes

Nicolaas A. Stolwijk,\* Christian Heddier, Manuel Reschke, Manfred Wiencierz, Joachim Bokeloh, and Gerhard Wilde

Institut für Materialphysik and Sonderforschungsbereich 458, University of Münster, D-48149 Münster, Germany

## Supporting Information

**ABSTRACT:** We measured glass transition temperatures  $T_g$  as a function of the salt concentration in polymer electrolyte systems consisting of poly(ethylene oxide) (PEO) complexed either with sodium iodide (NaI) or lithium bis(trifluorosulfonylimide) (LiTFSI). At homologous compositions,  $T_g$  of PEO–NaI is found to be generally larger than that of LiTFSI. The present  $T_g$  values are markedly higher than previously reported reference data. Also the observed nonlinear concentration dependence differs from earlier studies. These findings are tentatively attributed to the more stringent preparation and measuring conditions maintained in the present work, thereby keeping organic solvent residues and water contamination at low levels. Also the high molecular weight of the polymer may have some influence. The measurements were performed by differential scanning calorimetry after quenching from the melt. We find that *ex situ* immersion quenching in liquid nitrogen leads to lower degrees of crystallinity than *in situ* quenching in the calorimeter environment. In addition, the strong decrease of the crystallinity with increasing salt content gives rise to pronounced steps in the heat capacity near  $T_g$  for the more concentrated electrolytes.



## INTRODUCTION

Since their discovery in 1973,<sup>1</sup> solid-like polymer electrolytes (SPEs) have been extensively investigated. These complexes, consisting of a polar polymer matrix and a metal salt with sufficiently low lattice energy, exhibit a combination of properties which make them interesting for application in batteries and other electrochemical devices.<sup>2</sup> Most published studies deal with the easy-to-prepare polyether/alkali-metal complexes, which provide the technologically necessary mechanical flexibility as well as a fairly high ionic conductivity in the amorphous phase.<sup>3,4</sup>

In the case of polymer electrolytes, both the ionic mobility and the (microscopic) viscosity depend on the flexibility of the polymer chain segments, which is characterized by the glass transition temperature  $T_g$ . This renders it difficult to tailor/optimize the mechanical and ion-conduction properties separately. Rather it has been generally observed that an increase of the salt concentration to enhance the number of the charge carriers is counteracted by a decrease of the ionic mobility, which is due to the stiffening of the electrolyte material and accompanied by a significant increase of  $T_g$ .<sup>5</sup> However, despite the fact that the glass transition temperature may be viewed as a crucial parameter for polymer electrolytes, the number of systematic studies relating  $T_g$  to salt concentration (see, e.g., refs 6–10) is astonishingly small.

Previously published work at our laboratory dealt with ionic transport in PEO–NaI polymer electrolytes made up of poly(ethylene oxide) (PEO) complexed with sodium iodide.<sup>11–14</sup> For a series of compositions PEO<sub>y</sub>NaI, specified by

the EO/Na ratio  $y$  running from 10 to 1000, we measured the diffusivity of cations and anions with the radiotracers <sup>22</sup>Na and <sup>125</sup>I, respectively, over a wide temperature range (70–200 °C) in the (highly viscous) melt. Combining these data with the dc ionic conductivity  $\sigma_{dc}$  deduced from impedance spectroscopy, a virtually complete picture of mass and charge transport was obtained. To allow for a simultaneous evaluation of the three sets of experimental data for each composition,  $\sigma_{dc}$  was converted into the charge diffusivity  $D_\sigma$  with the aid of the Nernst–Einstein equation. On reasonable grounds, the employed transport model was assumed to rely on the occurrence of charged single ions ( $\text{Na}^+, \text{I}^-$ ) which may associate to form neutral pairs ( $\text{NaI}^0$ ). Specifically, the formal description was based on an expression for the pair fraction  $r_p$ , resulting from the mass action law, and on the “true” diffusivity of the individual mobile species given by

$$D_x = D_x^0 \exp[-B_x/(T - T_0)] \quad (1)$$

where the index “x” stands for  $\text{Na}^+$ ,  $\text{I}^-$ , or  $p = \text{NaI}^0$ . This Vogel–Tammann–Fulcher- (VTF-) like equation depends on the particle-specific parameters  $B_x$  and  $D_x^0$ , subject to model-specific constraints,<sup>11,15</sup> as well as on the common parameter  $T_0$  denoting the “zero mobility temperature” or “ideal” glass transition temperature.<sup>16</sup>

Received: August 12, 2013

Revised: October 11, 2013

Published: October 23, 2013

In principle,  $T_0$  can be assessed by fitting of the experimental data, as was done in earlier work at our laboratory.<sup>11,12</sup> However, the accurate determination of  $T_0$  is not only affected by experimental error but also suffers from intercorrelations with the fitting of the VTF parameters  $B_x$  in a least-squares minimization procedure. The latter drawback is usually pronounced in ionic transport studies on polymer electrolytes because of the narrow  $T$ -ranges involved and the weak curvatures of the pertaining data when plotted in an Arrhenius diagram. Therefore, it would be beneficial to have an independent estimate of the  $T_0$  value.

Both  $T_0$  and  $T_g$  are indicative of the chain-segment flexibility of the amorphous polymeric substance under consideration. More specifically, in early studies of the shear viscosity and ion conductivity it was found that  $T_0 \approx T_g - 50$  K may hold as an empirical rule for a broad spectrum of soft disordered materials.<sup>17–19</sup> In our recent work, we are dealing with different compositions within one and the same salt-in-polymer system, e.g., PEO<sub>*y*</sub>NaI with varying  $y$ .<sup>14</sup> In this case, it seems even more justified to assume that  $T_0$  and  $T_g$  are closely correlated, e.g., by the expression  $T_0(y) \approx T_g(y) - \Delta_0$ , where  $\Delta_0$  designates a constant  $T$ -shift independent of  $y$ . Thus, measuring  $T_g(y)$  using thermal analysis would enable us to estimate  $T_0(y)$  to a good approximation. This can be done either by taking a fixed value for  $\Delta_0$  (e.g., 50 K) or by adjusting  $\Delta_0$  in a overall fitting procedure that includes the transport data of all compositions.<sup>14</sup>

The present article reports the results of caloric  $T_g$  measurements on the systems PEO–NaI and PEO–LiTFSI (lithium bis(trifluoromethylsulfonyl)imide) upon quenching from the melt. PEO–NaI is a salt-in-polymer complex with model character and closely connected with the discovery of polymer electrolytes as a individual class of materials.<sup>1</sup> As indicated above, PEO<sub>*y*</sub>NaI complexes reveal a pronounced ion-pairing tendency, which strongly depends on salt concentration in the dilute range ( $y \geq 30$ ).<sup>14</sup> The PEO–LiTFSI system has attracted much attention because of some useful properties with regard to applications in lithium batteries. Specifically, PEO<sub>*y*</sub>LiTFSI complexes show little or no pair formation and a higher conductivity than PEO<sub>*y*</sub>NaI complexes with the same composition parameter  $y$ , which relates to the bulky nature of the TFSI anion.<sup>13</sup> In general, polymer electrolytes of low salt concentration are of fundamental scientific interest, as complications due to phase separation and high ion densities are avoided.

The  $T_g$  data obtained in this work cover a wide range of salt concentrations  $C_s$  which run from nominally zero to about 2.4 mol/L. The reliability of the data is sustained by comparative tests at different quenching rates and temperatures. We find a surprisingly strong increase of  $T_g$  with increasing  $C_s$ , which is much steeper than for published data on the same system.<sup>6,20</sup> The observed  $C_s$ -dependence is also stronger than reported for similar PEO-based systems with other alkali-metal salts. At higher salt concentrations  $T_g$  was found to be fairly constant. The results will be discussed with regard to phase separation, degree of crystallization, and contamination effects.

## ■ EXPERIMENTAL SECTION

**Materials and Preparation.** Appropriate amounts of PEO with a molecular weight of  $8 \times 10^6$  g/mol (Aldrich<sup>21</sup>) and either NaI (>99 wt %, Grüssing) or LiN(CF<sub>3</sub>SO<sub>2</sub>)<sub>2</sub> (LiTFSI, 99.95%, Sigma-Aldrich) were dried under continuous vacuum pumping at elevated temperature and subsequently homogeneously dissolved in extra dry acetonitrile (Acros

Organics, >99.95%, water content <0.01%, evaporation residue <0.001%). After evaporation of the solvent under high vacuum (HV,  $10^{-5}$  hPa) at 100 °C using cryogenic traps, the already very dry and tough SPE material was cut in tiny pieces and again subjected to a HV treatment at 50 °C for 24 h. In this way, solvent-free complexes of different composition were obtained: PEO<sub>*y*</sub>NaI with  $y = 10, 20, 30, 60, 120, 250, 500$ , or 1000 and PEO<sub>*y*</sub>LiTFSI with  $y = 20, 60, 250$ , or 1000. Great care was taken to avoid contact with ambient atmosphere. In analysis by pulsed-field-gradient nuclear magnetic resonance (PFG-NMR, not shown here), no <sup>1</sup>H resonance attributable to water or acetonitrile could be detected. Considering that all preparation steps were either carried out in a nitrogen-filled glovebox ( $H_2O < 1$  ppm) or under continuous pumping in the HV range, the water contamination of the SPEs is assumed to be at the 10 ppm level or below.

**Electrolyte Characterization.** The prepared materials were generally characterized by Archimedes-type mass density measurements and differential scanning calorimetry (DSC) using PerkinElmer DSC-7 equipment. The mass density enters the calculation of the salt concentration per unit volume. In DSC analysis over the temperature range from room temperature to 200 °C, the only feature in second and multiple heating/cooling cycles was the endothermic peak near 67 °C due to the melting of PEO. We found no indications of precipitation, in agreement with literature data on PEO–NaI (see, e.g., Fauteux et al.<sup>22</sup>) and PEO–LiTFSI<sup>23</sup> but in contrast to observations for PEO–MI complexes with larger alkali metal cations ( $M = K, Rb$ , and  $Cs$ ).<sup>24</sup> The reliable quality of all sample materials was confirmed by their systematic and reproducible behavior as a function of temperature and composition in conductivity measurements with electric impedance spectroscopy<sup>13</sup> and in diffusion experiments using radiotracers (PEO–NaI<sup>14</sup>) or PFG-NMR analysis (PEO–LiTFSI<sup>25</sup>).

**Measurements of the Glass Transition Temperature.** To determine  $T_g$  of amorphous PEO<sub>*y*</sub>NaI and PEO<sub>*y*</sub>LiTFSI complexes, melt-quenched specimens were thermally analyzed by using a PerkinElmer Diamond DSC calorimeter with liquid nitrogen (LN<sub>2</sub>) cooling. For *ex situ* quenching, approximately 10 mg of substance was encapsulated in a standard-type aluminum DSC pan under N<sub>2</sub> glovebox atmosphere and subsequently enclosed in a custom-built aluminum quenching capsule of low (thermal) mass. In the course of the experiments, the prototype capsule was replaced by an improved version of smaller size and mass. Following an annealing treatment in an oil-bath thermostat for 30 to 45 min at a preset quenching temperature ( $T_q$ ) in the range 100–215 °C, the capsule was immersed in LN<sub>2</sub> under continuous agitation and finally left there at 77 K. Mean quenching rates were estimated to be in the range 1500–3000 K/min, depending on the mass of the employed capsule. Within 60 min after this *ex situ* quenching procedure, the DSC pan with the sample was mounted in the Diamond DSC calorimeter that was precooled at –80 °C, and kept at this temperature for typically 20 min. During mounting of the pan in the open measurement chamber a small temperature increase of 10–15 °C could not be avoided. Thus, *ex situ* quenching in conjunction with further *in situ* cooling constitutes the *first cooling cycle*. Then the glass transition was monitored by the occurrence of an endothermic event during heating across the melt transition up to 150 °C at a rate of 10 °C/min (*first heating cycle*). After application of a baseline correction,  $T_g$  was determined from the half-height point of the heat capacity change in the thermogram (“half- $c_p$  method”).

To check the reproducibility of  $T_g$ , the DSC measurement was repeated with a *second cooling cycle* from 150 to –80 °C inside the calorimeter followed by a stabilization time of typically 20 min and a *second heating cycle*. The second cooling cycle, also denoted as “*in situ* quenching”, immediately followed the first heating cycle, i.e., without holding time at 150 °C. It was performed at a nominal rate of –20 °C/min, which at lower temperatures was close to or even exceeded the maximum cooling rate physically/technically achievable under the given conditions. Generally, the differences between the consecutive *ex situ* and *in situ*  $T_g$  values were about 1 °C or less. In most cases, the whole measurement including the quenching procedure was repeated with multiple samples of the same composition. The corresponding variations in  $T_g$  were typically 2 °C or less. In the case of PEO–NaI,

the influence of the *ex situ* quenching temperature was investigated, i.e., by changing  $T_q$  for specimens of equal composition.

## RESULTS

**Phase Behavior.** Figure 1 displays the DSC thermograms of a PEO<sub>10</sub>NaI sample (dashed line) and a PEO<sub>20</sub>LiTFSI

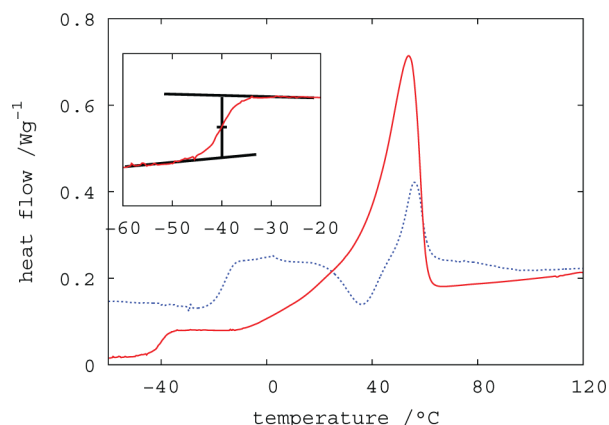


**Figure 1.** DSC thermograms of PEO<sub>10</sub>NaI (dashed line) and PEO<sub>20</sub>LiTFSI (solid line) electrolytes measured upon heating at 10 °C/min after *ex situ* quenching from 215 °C.  $T_g$  is determined by the half- $c_p$  procedure, as schematically demonstrated by the inset.

sample (solid line) that were both monitored during the first heating after LN<sub>2</sub> immersion quenching from 215 °C. At this temperature the complexes are fully melted, in accordance with the corresponding locations in the respective phase diagrams. For PEO<sub>10</sub>NaI and the other compositions of this system, this is readily verified by the phase diagram in Figure 2 that was

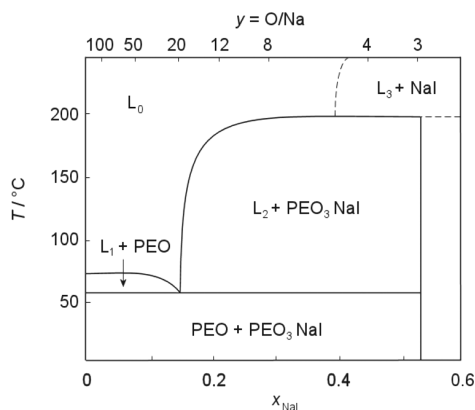


**Figure 2.** Phase diagram of the PEO–NaI system, as redrawn and adapted from the work of Fauteux et al.<sup>3,22</sup> The salt fraction  $x_{\text{NaI}}$  (lower  $x$ -axis) is based on weight ratios. The oxygen-to-sodium ratio O:Na (upper  $x$ -axis) equals the composition parameter  $y$ .

redrawn and adapted from the work of Fauteux et al.<sup>3,22</sup> Here, the single-phase melt region  $L_0$  designates the equilibrium state of the electrolytes before quenching. A similar situation prevails for PEO<sub>20</sub>LiTFSI and the related, more dilute compositions, as may be checked with the PEO–LiTFSI phase diagrams found in the literature.<sup>6,26</sup>

In Figure 1, the PEO<sub>20</sub>LiTFSI thermogram (solid line) shows two endothermic events in the depicted  $T$ -range, i.e., a glass transition at  $-40$  °C followed by a melt transition near  $55$  °C. Thus, there is no clear sign of incipient crystallization between

these events. The distinct heat-flow step at the lower temperature allows for a reliable determination of  $T_g$  by the half- $c_p$  procedure, as illustrated by the inset of Figure 1. From the area under the melt peak, the degree of crystallinity can be calculated (see below).

The dashed curve in Figure 1 is representative of PEO<sub>10</sub>NaI. It exhibits a large step in the heat capacity ( $\Delta c_p$ ) at  $-16$  °C marking  $T_g$ . In this case, the maximum due to melting of the polymer at  $55$  °C is preceded by the exothermic crystallization event near  $35$  °C. Not only the large value of  $\Delta c_p$  but also the similar sizes of the crystallization and melting peak point to a low degree of crystallinity in the quenched state.

**Crystallinity and Quenching Efficiency.** The crystallinity  $\chi_c$  of melt-quenched SPE samples is usually deduced from the DSC thermograms upon heating from the supercooled to the equilibrium melt phase. Specifically,  $\chi_c$  was obtained by using the expression

$$\chi_c = \frac{\Delta H}{\Delta H_{\text{PEO}} f_{\text{PEO}}} \quad (2)$$

where  $\Delta H$  in J/g denotes the difference between the melting endotherm and the crystallization endotherm (if observed). In addition,  $\Delta H_{\text{PEO}}$  is the enthalpy of fusion of fully crystalline PEO ( $196.4$  J/g<sup>27</sup>) and  $f_{\text{PEO}}$  is the PEO weight fraction of the sample.

Figure 3 shows the crystallinity as a function of the reduced salt concentration for both systems initially equilibrated at 215

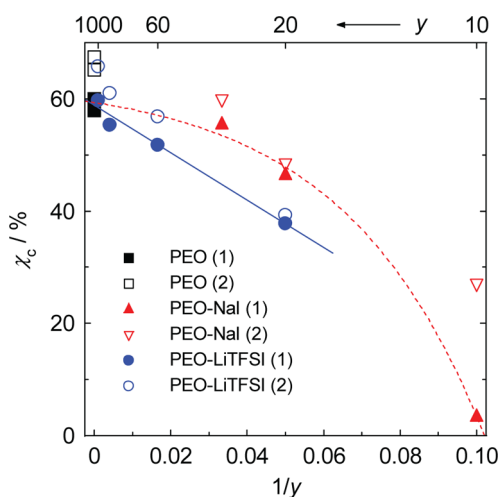


**Figure 3.** Crystallinity  $\chi_c$  of PEO <sub>$y$</sub> NaI and PEO <sub>$y$</sub> LiTFSI electrolytes as a function of the reduced salt concentration  $1/y$ . A distinction is made between data obtained during the first (closed symbols) and second (open symbols) heating cycle (i.e., after *ex situ* and *in situ* quenching, respectively). Solid and dashed line serve to guide the eye.

°C. In the case of PEO <sub>$y$</sub> LiTFSI we observe a virtual linear decrease of  $\chi_c$  with  $1/y$  from about 60% for pure PEO to about 40% for  $1/y = 0.05$ , as indicated by the straight line fitted to the data of the first cycle. For PEO <sub>$y$</sub> NaI,  $\chi_c$  of the first cycle falls from values near 60% for  $1/y = 0$  down to about 3.5% for  $1/y = 0.1$ . Thus, the PEO<sub>10</sub>NaI complex was quenched to a predominantly glassy state with a frozen-in “amorphicity” of close to 100%. Apparently, the crystallization kinetics in salt-rich polymer electrolytes is much slower than in dilute ones. The dashed line fitted to the PEO <sub>$y$</sub> NaI data is of exponential shape but only serves to guide the eye.



The  $\chi_c$  values obtained after LN<sub>2</sub> immersion quenching from 215 °C (1st heating) are generally lower than those resulting from DSC quenching from 150 °C (2nd heating). This is seen in Figure 3 by comparing the closed and open symbols for both electrolyte systems. For  $1/y \leq 0.05$ , the differences  $\Delta\chi_c$  between the two quenching methods appear to decrease with increasing salt concentration and thus with decreasing crystallinity (see above), i.e.,  $\Delta\chi_c \approx 7\%$  for pure PEO and  $\Delta\chi_c \approx 1.5\%$  for PEO<sub>20</sub>LiTFSI. This demonstrates that the present *ex situ* quenching procedure is more effective than the *in situ* one. In addition, the findings for  $\Delta\chi_c$  corroborate the preceding statement concerning the more rapid crystallization in salt-poor electrolytes. However, for PEO<sub>10</sub>NaI there is a great disparity of 22% in  $\chi_c$  between the two quenching methods. This relates to a substantial crystallization during the second cooling (directly following the first heating), as also found for all other electrolytes. It should be noted that PEO<sub>10</sub>NaI is the only complex that exhibited a clear crystallization event during the first heating (cf. Figure 1).

**Glass Transition Temperatures.** Figure 4 shows the  $T_g$  data for PEO<sub>y</sub>NaI obtained by quenching from different *ex situ*

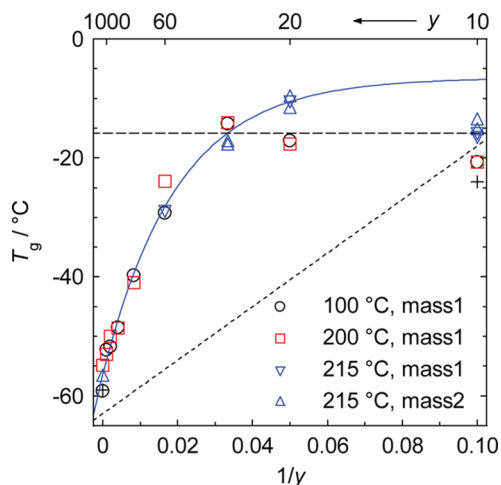


**Figure 4.** Glass transition temperature  $T_g$  of PEO<sub>y</sub>NaI complexes as a function of the reduced salt concentration  $1/y$  measured upon heating at 10 °C/min after quenching at different temperatures  $T_q$ , as indicated. The solid line represents the best fit by eq 3 to all data for  $1/y \leq 0.033$  and those for  $1/y = 0.05$  with  $T_q = 215$  °C (triangles). The coarsely dashed line represents a constant value ( $T_g = -15.8$  °C), as may be expected for quenching within the  $L_2$  + PEO<sub>3</sub>NaI phase region (cf. Figure 2). Previously published data are reproduced by the finely dashed line<sup>20</sup> and the crosses.<sup>28,29</sup>

equilibration temperatures  $T_q$  as a function of the reduced salt concentration  $1/y$  (open and closed symbols). Every data point represents the mean value over multiple samples including in each case two heating cycles (*ex situ* and *in situ* quenching). The experimental error is typically given by  $\pm 2$  °C.

Initially, a relatively low value of  $T_q = 100$  °C within the melt phase region  $L_0$  was chosen, in order to promote fast quenching (cf. Figure 2). It is seen that the data (open circles) exhibit a monotonic steep increase up to  $1/y \approx 0.033$ , beyond which  $T_g$  only varies within a limited range between about  $-15$  and  $-20$  °C. Qualitatively, this seems to comply with a crossover of the liquidus line in the phase diagram ( $L_2$  in Figure 2), since it may be expected that  $T_g$  will be independent of  $y$  in the two-phase area between the eutectic and the line compound PEO<sub>3</sub>NaI.

However, a quantitative disparity becomes manifest because of the difference between the position of the kink in  $T_g$  ( $y \approx 30$ ) and the location of the liquidus in the phase diagram ( $y \approx 20$  at  $T_q = 100$  °C).

To verify and supplement our initial results, we performed another series of experiments with a distinctly higher quenching temperature. Choosing  $T_q = 200$  °C enables us to avoid the two-phase region  $L_2$  + PEO<sub>3</sub>NaI in Figure 2 also for the salt-rich compositions ( $y \leq 20$ ), provided that the quenching procedure is rapid enough. The resulting  $T_g$  values are plotted in Figure 4 as open squares. For  $y \geq 30$ , circles and squares agree within experimental error, indicating that in this dilute composition range also quenching from a relatively high temperature (200 °C) proceeds sufficiently fast to avoid phase separation and the concomitant compositional changes in the two-phase regions  $L_1$  + PEO and PEO + PEO<sub>3</sub>NaI crossed and attained in the low-temperature regime, respectively. However, also these further  $T_g$  data for PEO<sub>20</sub>NaI and PEO<sub>10</sub>NaI (squares,  $T_q = 200$  °C) agree with the initial ones (circles,  $T_q = 100$  °C).

The reasons for this observation may be 2-fold. First, quenching may not be efficient enough to suppress the PEO<sub>3</sub>NaI precipitation upon crossing the liquidus line  $L_2$ , i.e., entering the two-phase area (cf. Figure 2). Second, it seems conceivable that the liquidus line  $L_2$  is rather inaccurate, so that a quenching temperature of 200 °C could still be within the “true”  $L_2$  + PEO<sub>3</sub>NaI region for the high salt concentrations of interest. The latter hypothesis was checked by further experiments, in which  $T_q$  was raised to 215 °C.

In Figure 4, the data representing  $T_q = 215$  °C are plotted as open and closed triangles. These symbols discriminate between two versions of the quenching capsule, having either a higher (downward-triangle) or a lower (upward-triangle) mass. However, no significant dependence on the capsule mass (size) is observed. For dilute compositions ( $1/y \leq 1/30$ ), the  $T_g$  data from  $T_q = 215$  °C agree with those from the lower quenching temperatures within experimental error (cf. Figure 4). For PEO<sub>20</sub>NaI, however, the new  $T_g$  values (close to  $-10$  °C; triangles) are higher than the initial ones (ca.  $-17$  °C; circle and square). Apparently, the  $T_g$  data obtained by quenching from 215 °C follow the course of  $T_g$  with  $1/y$  for the lower salt concentrations, as indicated by the solid line in Figure 4. In fact, all these data are well described by the empirical expression (solid line)

$$T_g = T_{g0} + \Delta_T [1 - \exp(-a/y)] \quad (3)$$

where the parameters  $T_{g0} = -56.5 \pm 0.7$  °C,  $\Delta_T = 49.7 \pm 1.9$  °C, and  $a = 51.7 \pm 5.1$  result from least-squares fitting. In this equation,  $T_{g0}$  denotes the glass transition temperature of pristine PEO ( $1/y = 0$ ), while  $\Delta_T$  and  $a$  characterize the amplitude and the relative change rate of  $T_g - T_{g0}$  with salt concentration.

For PEO<sub>10</sub>NaI, the  $T_g$  values upon quenching from 215 °C fall below those of PEO<sub>20</sub>NaI and they are on the same level as the PEO<sub>30</sub>NaI value (see closed triangles in Figure 4). This may indicate that even with the capsule of low mass quenching was not fast enough to suppress the PEO<sub>3</sub>NaI precipitation upon crossing the two-phase region between about 200 and 60 °C. Nevertheless, choosing 215 °C for  $T_q$  instead of 200 or 100 °C obviously leads to higher glass transition temperatures for compositions with  $1/y \geq 1/30$ .

The  $T_g$  data of PEO<sub>y</sub>LiTFSI are displayed in Figure 5. All data result from  $T_q = 215$  °C as initial quenching temperature.

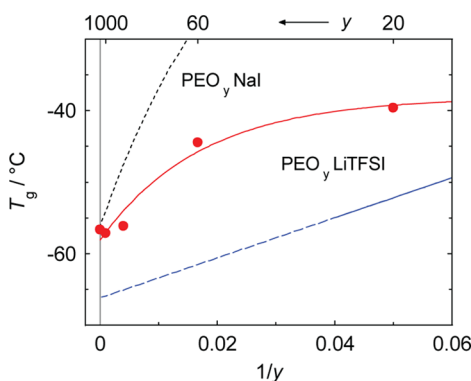


**Figure 5.** Glass transition temperature  $T_g$  of  $\text{PEO}_y\text{LiTFSI}$  complexes as a function of the reduced salt concentration  $1/y$  measured upon heating at  $10^\circ\text{C}/\text{min}$  after quenching from  $T_q = 215^\circ\text{C}$ . The solid line represents the best fit by eq 3 to all data. Previously published data are reproduced by the low straight line,<sup>6,30</sup> of which the dashed part indicates an extrapolated range. The finely dashed line represents the  $T_g$  data of  $\text{PEO}_y\text{NaI}$  (cf. Figure 4).

As indicated before, subsequent *ex situ* and *in situ* experiments agree within experimental error. In fact, the plotted data represent averages of multiple samples with two heating cycles each. The data are fitted by eq 3 (solid line) yielding the following best parameter values:  $T_{g0} = -58.1 \pm 1.4^\circ\text{C}$ ,  $\Delta_T = 20.0 \pm 3.2^\circ\text{C}$ , and  $a = 57.8 \pm 26.9$ .

## DISCUSSION

**Comparison with Literature Data.** Previous  $T_g$  data for the  $\text{PEO-NaI}$  system have been reported by Minier et al.<sup>20,31</sup> Their data are described by the linear equation  $T_g = T_{g0} + 450(1/y)$ ,<sup>20</sup> which includes the value of pure PEO,  $T_{g0} = -63^\circ\text{C}$ , for which the original paper refers to the literature.<sup>32</sup> Figure 4 shows that these early data, represented by the finely dashed line, differ considerably from the present ones, both quantitatively and qualitatively. We observe in our work not only markedly higher  $T_g$  values, with a maximum difference of about  $32^\circ\text{C}$  near  $1/y = 0.04$ , but also a pronounced nonlinear dependence on the salt concentration in the dilute range.

It should be mentioned, however, that only two compositions of Minier et al.<sup>31</sup> ( $y = 10, 24$ ) fall into the range depicted in Figure 3. Furthermore, their  $T_g$  value of  $\text{PEO}_{10}\text{NaI}$  was found to vary from  $-3$  to  $-23^\circ\text{C}$  upon changes in  $T_q$  from  $127$  to  $172^\circ\text{C}$ , however, in a nonmonotonic manner. For the composition with  $y = 24$ , the  $T_g$  value differed by  $25^\circ\text{C}$  between slow and fast cooling.<sup>31</sup> Other publications on  $\text{PEO-NaI}$  report  $T_g = -24^\circ\text{C}$  for  $y = 10$  and  $T_g = -59^\circ\text{C}$  for pure PEO.<sup>28,29</sup> These data are shown by the crosses in Figure 4. Obviously, the value for  $\text{PEO}_{10}\text{NaI}$  (cross) is even smaller than that of Minier et al.<sup>31</sup> (dashed line).

Also for  $\text{PEO-LiTFSI}$ , the previously published  $T_g$  data fall distinctly below the present results. This is obvious from the position of the lowest line in Figure 5 reproducing the results of Lascaud et al.<sup>6,30</sup> Only their compositions with  $10 \leq y \leq 24$  represented by the solid line segment with slope  $2.8^\circ\text{C}/\text{mol } \%$ <sup>6,30</sup> are in the range of the present study. The dashed line segment is a mere extrapolation to zero salt concentration and thus not supported by experimental data. Altogether, the data constellation for  $\text{PEO-LiTFSI}$  in Figure 5 is similar to that of  $\text{PEO-NaI}$  in Figure 4. Specifically, the largest difference between the old and new  $T_g$  data amounts to about  $16^\circ\text{C}$  near  $1/y = 0.03$ .

Lascaud et al. also measured  $T_g$  for more concentrated  $\text{PEO-LiTFSI}$  complexes, i.e., up to the very salt-rich composition with  $y = 0.5$ .<sup>6,30</sup> They observed a monotonic increase with increasing molar fraction of salt,  $x_{\text{salt}} = 1/(1+y)$ , up to a (near-)liquidus composition ( $x_{\text{salt}} \approx 0.4$ ,  $y = 1.5$ ) followed by a constant  $T_g$  of  $14^\circ\text{C}$  indicative of a two-phase region (liquid complex plus pure salt).<sup>6</sup> However, quenching temperatures are not mentioned in their work and the dependence of  $T_g$  on  $T_q$  was apparently not explored.

Other  $\text{PEO-salt}$  systems investigated for their phase behavior and glass transitions include  $\text{LiCF}_3\text{SO}_3$ ,<sup>33,34</sup>  $\text{MSCN}$  (with  $M = \text{Li, Na, K, and Cs}$ ),<sup>35,36</sup>  $\text{LiClO}_4$ ,<sup>33</sup>  $\text{LiBPh}_4$ ,<sup>36</sup> and  $\text{MTFSI}$  (with  $M = \text{Na and K}$ ).<sup>30</sup> All these studies were carried out by Prud'homme and co-workers like that on  $\text{PEO-LiTFSI}$ .<sup>6,30</sup> The range of examined compositions typically extended from  $y = 24$  to  $y = 1.5$ , similar to  $\text{PEO-LiTFSI}$ , so that the extreme low-concentration regime including pristine PEO was not covered by these early data. In the dilute range of all these electrolytes, the increase of  $T_g$  with salt concentration was rather modest, of linear type, and never exceeded a slope of  $6.7^\circ\text{C}/\text{mol } \%$ .<sup>6</sup> This figure has to be compared with the slope  $S_g$  of the  $T_g$ -versus- $1/y$  plots in Figures 4 and 5, containing the aforementioned literature values for  $\text{PEO-LiTFSI}$  ( $2.8^\circ\text{C}/\text{mol } \%$ ) and  $\text{PEO-NaI}$  ( $4.5^\circ\text{C}/\text{mol } \%$ ).<sup>20</sup>

Obviously, distinctly higher  $T_g$  increase rates are observed for the present strongly diluted  $\text{PEO-NaI}$  and  $\text{PEO-LiTFSI}$  complexes. For  $\text{PEO-NaI}$ , this is quantitatively confirmed by calculating the slope of eq 3 as  $S_g \equiv dT_g/d(1/y) = a\Delta_T \exp(-a/y)$ , where for dilute compositions  $1/y$  does not significantly differ from  $x_{\text{salt}} = 1/(1+y)$ . Indeed, in the low-concentration limit we have  $S_g = 25.7^\circ\text{C}/\text{mol } \%$  while for  $1/y = 0.02$  our data yield  $S_g = 9.1^\circ\text{C}/\text{mol } \%$ . However, for  $1/y = 0.033$  and  $0.05$  the present increase rate reduces to  $4.6$  and  $1.9^\circ\text{C}/\text{mol } \%$ , respectively. The latter  $S_g$  values comply with the increase rates reported in the literature for comparable composition domains. Yet a disparity remains, since  $\text{PEO-NaI}$  exhibits the “common” low  $T_g$  increase for  $T_g$  values only in the range from  $-20$  to  $-10^\circ\text{C}$  (Figure 4), whereas the related systems mentioned above show a similar behavior over longer  $T_g$  intervals extending to temperatures down to about  $-55^\circ\text{C}$ .

**Comparison of  $\text{PEO-NaI}$  with  $\text{PEO-LiTFSI}$ .** For the two systems examined, the actual  $T_g$  data are generally higher than the previously published ones. However, what remains in both cases is that  $T_g$  of  $\text{PEO-NaI}$  exceeds that of  $\text{PEO-LiTFSI}$  for the same salt concentration over fairly wide composition ranges. It is known that the alkali metal ions  $\text{Na}$  and  $\text{Li}$  similarly coordinate to the oxygen atoms in the polymer chains leading to conformational constraints of the PEO segments involved in cation binding. The concomitant reduction of polymer flexibility is accompanied by an increase of  $T_g$ . Probably, the differences in  $T_g$  induced by  $\text{Na}$  and  $\text{Li}$  coordination are small, since it was observed that the ion conductivity of  $\text{PEO}_{30}\text{MI}$  electrolytes with  $M = \text{Li, Na, K, Rb, or Cs}$  coincides over broad temperature ranges in the amorphous phases<sup>24</sup> (cf.  $L_0$  region in Figure 2). Consequently, the disparity in  $T_g$  between  $\text{PEO-NaI}$  and  $\text{PEO-LiTFSI}$  essentially arises from the distinct anions involved. Specifically, the bulky TFSI ions may more efficiently prevent dense packing of polymer segments than the comparatively small iodine ions and thus have a stronger plasticizing effect.<sup>33</sup>

The present glass transition temperatures of  $\text{PEO-NaI}$  and  $\text{PEO-LiTFSI}$  exhibit similar behavior as a function of salt

concentration, which is empirically described by eq 3. The relative change per unit of reduced concentration,  $(T_g - T_{g0})^{-1} d(T_g - T_{g0})/d(1/y) = a/(\exp(a/y) - 1)$ , is given by the dimensionless parameter “ $a$ ” in eq 3. It is found by fitting that the numerical values of this parameter for PEO–NaI ( $a = 51.7$ ) and PEO–LiTFSI ( $a = 57.8$ ) are not too different. By contrast, the difference in  $\Delta_T$  is quite large, 49.7 °C versus 20.0 °C, which, according to the discussion above, mainly reflects the dissimilar properties of the anions. Altogether, this quantitative analysis seems more reliable for PEO–NaI than for PEO–LiTFSI, i.e., because of the larger body of experimental data and the wider composition range of the former system.

**Composition Dependence of  $T_g$ .** The present fitting result for PEO–NaI (cf. eq 3) only slightly differs from a similar expression previously used for the evaluation of ion transport data.<sup>14</sup> As indicated in the Introduction, we utilized the experimental  $T$ -dependence of  $T_g$  for a simultaneous fit of all PEO<sub>*y*</sub>NaI transport data (diffusivity of Na and I as well as the charge diffusivity  $D_o$ ) comprising six compositions in the  $y$ -range from 30 to 1000. Thus, based on the empirical rule<sup>17–19</sup> that  $T_g$  and the VTF parameter  $T_0$  only differ by a  $y$ -independent constant, i.e.,  $T_0(y) \approx T_g(y) - \Delta_0$ , all measured diffusion coefficients were well reproduced with the adjusted best value  $\Delta_0 = 44 \pm 3$  K.<sup>14</sup> This finding supports the reliability of the  $T_g$  data obtained in the present work. In particular, the steep increase of  $T_g$  with increasing salt concentration for PEO–NaI (cf. Figure 4) appears to be reflected by corresponding changes in the ionic diffusivity (cf. eq 1).

For polymer electrolytes, diverse  $T_g$  behavior as a function composition has been reported in the literature. A simple linear dependence on the salt concentration was mentioned before regarding the work of Minier et al.<sup>20,31</sup> and the Prud’homme group.<sup>6</sup> On the other hand, LeNest et al.<sup>5</sup> observe for PEO of low molecular weight (1050, 2100, and 3800 g/mol) complexed with LiClO<sub>4</sub> a linear decrease of the *inverse* glass transition temperature, i.e.,  $1/T_g = 1/T_{g0} - 2.7 \times 10^{-4} C_s$  with  $C_s$  given in mol/L. Similar behavior was found for the same PEO materials without salt as a function of the urethane cross-link density. On the basis of their quantitative results, LeNest et al.<sup>3,5</sup> conclude that cations bound to the ether groups of PEO act as cross-links of reduced effectivity. It is noteworthy that these authors used *ex situ* quenching in LN<sub>2</sub>, like in the present work, with  $T_q = 100$  °C. We checked the above relationship by plotting our PEO–NaI and PEO–LiTFSI data as  $1/T_g$  versus  $1/y$ . However, for both systems a pronounced nonlinear behavior was observed, which does not agree with the findings on PEO–LiClO<sub>4</sub>.<sup>5</sup>

Kim et al.<sup>10,37</sup> have provided an equation for the composition dependence of  $T_g$  in polymer–salt systems which is based on changes in configurational entropy, using the ideas of DiMarzio and Gibbs<sup>38</sup> as well as Flory–Huggins theory.<sup>39</sup> This equation is nonlinear in  $x_{\text{salt}}$  and it predicts a  $T_g$  behavior globally similar to that observed in the present study. However, the use of Kim’s equation for the description of our data proved to be less successful, since it was not able to reproduce the strong curvature in  $T_g$  for small  $x_{\text{salt}} \approx 1/y$  values. This may not surprise, as the model of Kim et al.<sup>10,37</sup> involves several strong assumptions, e.g., (1) ion association is neglected, and (2) differences in the solvation of cations and anions are not taken into account. Both assumptions are questionable, since first, the impact of pair formation on ion transport, particularly in PEO–NaI, is found to be strong,<sup>13,14</sup> and second, the binding situation for cations and anions within the polymer matrix is

crucially different (see above). The development of an improved physical model is beyond the scope of the present article. We believe, however, that future evaluations should separately include the  $T_g$ -enhancing (stiffening) effect of cations, the  $T_g$ -lowering (plasticizing) effect of anions, and a possible influence of ion pairing.

For completeness it should be mentioned that exponential  $T_g$  behavior has been observed in polymers. Specifically, this concerns the dependence of  $T_g$  on the  $n$ -alkyl side chain length for a series of comblike structures, as reported by Reimschuessel.<sup>40</sup> In these cases,  $T_g$  decreases exponentially with increasing  $n$  up to a critical side chain length indicated by  $n_c$ . The expression given by Reimschuessel<sup>40</sup> bears resemblance to eq 3

**Possible Causes of Discrepancies in  $T_g$ . General Considerations.** Although the present glass transition temperatures of dilute polymer electrolytes are consistently higher than those reported in the literature, we can only speculate about the reasons for this finding. It is obvious that residual solvent and moisture in the samples may contribute to a lowering of  $T_g$ , as such contaminations act as plasticizer for the nominally solvent-free polymer–salt systems.<sup>41–43</sup> Also ineffective quenching caused by too low cooling rates may give rise to seemingly low  $T_g$  values, since then the precipitation of salt-rich crystalline phases cannot be prevented. In that case, the measured glass transition temperature has to be attributed to an amorphous phase which is more dilute in salt than the nominal composition of the quenched specimen. On the contrary, it is hard to conceive of preparative or experimental artifacts that would lead to a significant *increase* of  $T_g$ .

Small differences among  $T_g$  data on nominally identical samples may arise from experimental error including variations in composition and temperature within common tolerances. In addition, some scatter among the results from different studies may be due to differences in heating rate (10–40 °C/min) and the applied  $T_g$  evaluation method, i.e., as denoted by “half- $c_p$ ”, “point of inflection”, “onset value”, or some other keyword. However, the overall uncertainty from such sources may be estimated to be on the order of  $\pm 5$  °C in worst cases, which is still far below the discrepancies of up to 32 °C (PEO–NaI) and 16 °C (PEO–LiTFSI) between present and previous  $T_g$  data disclosed in this work.

**Effect of Polymer Specifications.** Differences in  $T_g$  may also be due to distinct specifications of the employed materials. In particular, molecular weight and purity of the polymer may be relevant features of the polymer–salt complexes. The PEO material in our work is characterized by a very high molecular weight ( $8 \times 10^6$  g/mol) and a production-related fraction of oxide particles (1.7 wt %).<sup>21,44</sup> In principle, this might explain that the present result for  $T_{g0}$  ( $-57 \pm 1$  °C) is slightly higher than some of the literature values (e.g.,  $-60$  to  $-65$  °C<sup>3,45</sup>). However, Wu et al.<sup>46</sup> report experimental  $T_g$  values for semicrystalline PEO to be in the range from  $-45$  to  $-60$  °C, which is based on the results of nine different original publications (for references, see Wu et al.<sup>46</sup>).

Also many other studies on polymer electrolytes are based on purchased PEO materials of high molecular weight, which always contains a small fraction of oxide particles.<sup>44</sup> This contamination is inherent to the manufacturing process but it is rarely mentioned in the experimental sections of published work.<sup>44</sup> However, several recent investigations show that the impact of added oxide particles on the glass transition and crystallinity of salt-in-PEO electrolytes is not significant.<sup>47,48</sup>



Data reported for  $\text{PEO}_{50}\text{AgCF}_3\text{SO}_3$  with varying amounts of  $\text{MgO}$  nanoparticles in the range from 1 wt % to 10 wt % show that  $T_g$  and  $\chi_c$  are essentially constant.<sup>47</sup> A similar result is obtained from a study on  $\text{PEO}_{15}\text{KI}$  for additions of nanosized  $\text{CeO}_2$  particles of up to 15 wt %.<sup>48</sup> Furthermore, also the particle size tends to be uncritical for  $T_g$  and  $\chi_c$  as indicated by the data on  $\text{PEO}_{25}\text{NaClO}_4$  with  $\text{ZrO}_2$ .<sup>48</sup>

Indirect evidence for the weak interaction between oxide nanofillers and the salt in SPE systems is obtained from ionic conductivity and diffusivity measurements. Several recent studies show that the admixture of different types and amounts of nanosized oxide particles changes the ion conductivity in the melt only to extents that are comparable with experimental error (e.g., 20%).<sup>44,49,50</sup> Similar is true for the diffusion coefficients of cations and anions as determined by PFG-NMR<sup>44</sup> or radiotracer techniques.<sup>50</sup> These studies include  $\text{PEO}_{20}\text{LiBETI}$  with 10 wt %  $\text{SiO}_2$  particles<sup>44</sup> and  $\text{PEO}_{60}\text{NaI}$  with 5 wt %  $\text{TiO}_2$  or 10 wt %  $\text{Al}_2\text{O}_3$  particles.<sup>50</sup> Altogether, the effect of 1.7 wt % oxide particles in the PEO material employed in this work seems negligible.

The early studies on  $\text{PEO-NaI}$  also used high-molecular-weight PEO, i.e., specified as  $9 \times 10^5$  g/mol<sup>31</sup> or  $5 \times 10^6$  g/mol.<sup>28</sup> Of the cited literature on polymer electrolytes, a direct measurement of  $T_g$  for pristine PEO is only reported by Przylusky and Wiczorek.<sup>28</sup> Their result,  $-59^\circ\text{C}$  (cf. Figure 4), is close to the present data. Therefore, it seems less plausible that the disparity in  $T_g$  from distinct studies on  $\text{PEO-NaI}$  is due to different material specifications. By contrast, the previous  $\text{PEO-LiTFSI}$  data are based on purified polymer material of relatively low molecular weight ( $\sim 4 \times 10^3$  g/mol<sup>6</sup>) like the other results of the Prud'homme group.<sup>30,33–36</sup> In these cases, a lowering of  $T_g$  with regard to high-molecular-weight material is in principle predicted by the Flory–Fox equation.<sup>51,52</sup> This effect is based on the relatively large number of chain end units in short-chain polymer matrices, which in turn leads to more free volume and higher segmental flexibility. Using quantitative data for other polymers,<sup>52</sup> also the magnitude of the  $T_g$ -difference for  $\text{PEO-LiTFSI}$  between present and previous<sup>6</sup> data could be rationalized by the differences in molecular weight. In addition, it has been observed for related  $\text{PEO/Li-salt}$  systems that the partial substitution of high-molecular-weight PEO with low-molecular-weight PEO leads to a lowering of  $T_g$ .<sup>53</sup> However, the question remains whether the chain length effect is able to explain the qualitative change in the  $T_g$  composition dependence as well, i.e., from linear to exponential-type (cf. Figures 4 and 5).

**Effect of Solvent and Water Residues.** To prepare their  $\text{PEO-NaI}$  complexes, Minier et al.<sup>31</sup> used the “solution and cast” procedure, after which the electrolyte film was outgassed under partial vacuum followed by a treatment in flowing argon. No information is given about sample handling. For similarly prepared  $\text{PEO-NaSCN}$  complexes, Lee and Christ<sup>54</sup> observed a  $T_g$ -dependence on salt concentration which is within a few percent of the Minier result. Interestingly, it is explicitly stated in their article<sup>54</sup> that “no precautions were taken to prevent contact with water vapor”. Thus, it seems plausible that the similarly low literature data reported for  $\text{PEO-NaI}$  and  $\text{PEO-NaSCN}$  have been influenced by the plasticizing effect of  $\text{H}_2\text{O}$  molecules.<sup>41</sup> By contrast, the preparation procedure for  $\text{PEO-LiTFSI}$  electrolytes by Lascaud et al.<sup>6</sup> is described in considerable detail. The reported use of high vacuum and elevated temperatures for solvent evaporation make it plausible that their polymer-salt mixtures were of high purity in the as-

prepared state. However, the authors provide little information about the avoidance of water contamination during sample handling.

The effect of solvent and water contamination was exemplarily monitored by rheological investigations on a related polyether-based system.<sup>55</sup> To this aim, a test sample prepared by the “solution and cast” method in air ambient was compared regarding its mechanical properties with reference material prepared by the standard high vacuum and glovebox procedures (see Experimental Section). After 3 days of ambient exposure, the storage modulus  $G'$  of the test sample at  $40^\circ\text{C}$  was found to be only about 60% of the reference value  $G'_0$ .<sup>55</sup> Gradually smaller and smaller decreases down to about 50% of  $G'_0$  were determined after 6 and 14 days of ambient exposure. A similar behavior was revealed by the zero shear viscosity.<sup>55</sup> These observations may be explained by the presence of residual acetonitrile in the test sample in conjunction with a continuous uptake of moisture from the air. We note that water absorption as a function of exposure time has been previously studied for PEO-based polymer electrolyte systems.<sup>56</sup> Our test experiment indicates that solvent and water contamination may lead to lower viscosities, which is closely connected to a decrease of  $T_g$ . Specifying the water or solvent content of polymer electrolytes (based on PEO of extremely high molecular weight) is not an easy task. At least no  $^1\text{H}$  signal related to water or acetonitrile was detected during PFG-NMR analysis (cf. Materials and Preparation). However, this point is not as critical as it seems, i.e., for the following reasons: (1) Quite high concentrations of water (0.05 molar fraction<sup>41</sup>) or organic solvent (several wt %<sup>42,43</sup>) are necessary to have a significant effect on  $T_g$ . Such concentrations are far beyond state-of-the-art contamination levels and thus certainly not contained in our samples. (2) The effect of water or organic solvents in noticeable amounts would lead to a decrease of  $T_g$ .<sup>41–43</sup> However, the main result of the present paper is a substantial increase of  $T_g$  compared to previous work. Therefore, our observations cannot be rationalized by artifacts due to solvent residues in our samples.

**Effect of Quenching Rate and Temperature.** In principle, the quenching temperature  $T_q$  and the quenching rate  $R_q$  are important parameters in measurements of  $T_g$ .  $T_q$  determines the equilibrium state of the sample at the onset of quenching, whereas  $R_q$  controls to which extent this initial state can be frozen in and thus to which extent phase separation can be avoided during the cooling-down procedure. It may be expected that  $R_q$  is more critical in the high- $T$  region where the ions are more mobile than at lower temperatures. In the case of  $\text{PEO-salt}$  complexes, a special feature is the (partial) crystallization of PEO. Usually, this phase transformation cannot be suppressed by *in situ* quenching, as also reported by others.<sup>6</sup> In our measurements, the corresponding exothermic events commonly occurred in the range from  $40^\circ\text{C}$  down to  $20^\circ\text{C}$ .

It should be emphasized that the present results for  $T_g$  do not critically depend on the quenching method. The data gained by *ex situ* and *in situ* quenching mutually agree in all cases (cf. Figures 4 and 5). There are only differences in the degree of crystallization  $\chi_c$ , which are generally small, except for  $\text{PEO}_{10}\text{NaI}$  (cf. Figures 3). Consequently, the disparity between our  $T_g$  values and the literature data cannot be explained by differences in the quenching rate.

By contrast, a dependence on the *ex situ* quenching temperature is found for  $\text{PEO}_y\text{NaI}$  with  $y \leq 20$  (cf. Figure



4), while it was not examined for PEO<sub>y</sub>LiTFSI. This dependence for concentrated PEO–NaI may relate to the position of the liquidus line  $L_2$  in Figure 2, as discussed in the section Glass Transition Temperatures. It is remarkable, however, that also for PEO<sub>10</sub>NaI and PEO<sub>20</sub>NaI the differences in  $T_g$  after consecutive *ex situ* ( $T_q = 215\text{ }^\circ\text{C}$ ) and *in situ* ( $T_q = 150\text{ }^\circ\text{C}$ ) quenching are within  $2\text{ }^\circ\text{C}$ . Apparently, the short time of residence in the melt phase between about 60 and 150  $^\circ\text{C}$  of roughly 14 min (first heating immediately followed by second cooling) is too short to establish a corresponding equilibrium state. This indicates that equilibration times may play a crucial role at moderate and lower quenching temperatures.

## CONCLUSIONS

The results of this study on the glass transition in the polymer-electrolyte systems PEO<sub>y</sub>NaI and PEO<sub>y</sub>LiTFSI can be summarized as follows:

- The present  $T_g$  values for salt concentrations below about 2.4 mol/L ( $y > 10$ ) are distinctly higher than comparable data reported in the literature.
- $T_g$  shows an exponential increase with increasing salt concentration in the highly diluted composition range. This clearly deviates from a linear dependence, as previously reported for PEO–NaI, PEO–LiTFSI, and other SPE systems.
- Ex situ* quenching using liquid nitrogen may lead to lower degrees of crystallinity than *in situ* quenching inside the calorimeter. As a result, bigger steps in the heat capacity at the glass transition are obtained, which facilitates the measurement of  $T_g$ .
- Upon quenching, the crystallinity of SPEs decreases with increasing salt concentration.

The reasons for the higher  $T_g$  data obtained in this work are not clear. In the case of PEO–NaI, the low levels of residual organic solvent and water contamination in our samples may be responsible for the determination of “true”  $T_g$  values representative of the pure binary salt-in-polymer complexes. For PEO–LiTFSI, the high molecular weight of the employed PEO material could at least partly explain the  $T_g$  increase with respect to the literature data. Further studies are needed to elucidate the composition dependence of the glass transition in polymer electrolytes.

## ASSOCIATED CONTENT

### Supporting Information

Additional DSC thermographs of PEO–NaI and PEO–LiTFSI complexes after melt quenching showing glass transitions and a table of storage module data on a related polyether-based electrolyte with solvent residues revealing effects of exposure to air ambient as a function of time. This material is available free of charge via the Internet at <http://pubs.acs.org>.

## AUTHOR INFORMATION

### Corresponding Author

\*(N.A.S.) E-mail: [stolwijk@uni-muenster.de](mailto:stolwijk@uni-muenster.de). Telephone: +49 (0)251 8339013. Fax: +49 (0)251 8338346.

### Notes

The authors declare no competing financial interest.

## ACKNOWLEDGMENTS

The authors thank J. Kösters, F. Call, and S. Knebel for help in the experiments as well as Dr. S. Passerini for fruitful

discussions. Financial support by the Deutsche Forschungsgemeinschaft within the Collaborative Research Centre SFB 458 is gratefully acknowledged.

## REFERENCES

- (1) Fenton, D. E.; Parker, J. M.; Wright, P. *Polymer* **1973**, *14*, 589–595.
- (2) Scrosati, B.; Vincent, C. A. *MRS Bull.* **2000**, *25* (3), 28–30.
- (3) Gray, F. M. *Solid Polymer Electrolytes*; VCH: New York, 1991.
- (4) Chandrasekhar, V. *Adv. Polym. Sci.* **1998**, *135*, 139.
- (5) Le Nest, J.-F.; Gandini, A.; Cheradame, H.; Cohen-Addad, J.-P. *Macromolecules* **1988**, *21*, 1117–1120.
- (6) Lascaud, S.; Perrier, M.; Vallee, A.; Besner, S.; Prud'homme, J.; Armand, M. *Macromolecules* **1994**, *27*, 7469–7477.
- (7) Cruickshank, J.; Hubbard, H.V.St.A.; Boden, N.; Ward, I. M. *Polymer* **1995**, *36*, 3779–3781.
- (8) Watanabe, M.; Nishimoto, A. *Solid State Ionics* **1995**, *79*, 306–312.
- (9) Onishi, K.; Matsumoto, M.; Shigehara, K. *Polym. Adv. Technol.* **2000**, *11*, 539–543.
- (10) Kim, J. H.; Min, B. R.; Won, J.; Kang, Y. S. *J. Phys. Chem. B* **2003**, *107*, 5901–5905.
- (11) Stolwijk, N. A.; Obeidi, Sh. *Phys. Rev. Lett.* **2004**, *93*, 125901–125904.
- (12) Stolwijk, N. A.; Wiencierz, M.; Obeidi, Sh. *Faraday Discuss.* **2007**, *134*, 157–169.
- (13) Stolwijk, N. A.; Wiencierz, M.; Heddier, Chr.; Kösters, J. *J. Phys. Chem. B* **2012**, *116*, 3065–3074.
- (14) Wiencierz, M.; Stolwijk, N. A. *Solid State Ionics* **2012**, *212*, 88–99.
- (15) Fögeling, J.; Kunze, M.; Schönhoff, M.; Stolwijk, N. A. *Phys. Chem. Chem. Phys.* **2010**, *12*, 7148–7161.
- (16) Ratner, M. A.; Shriver, D. F. *Chem. Rev.* **1988**, *88*, 109–124.
- (17) Ratner, M. A. In *Polymer Electrolyte Reviews*; MacCallum, J. R., Vincent, C. A., Eds.; Elsevier: London, 1987.
- (18) Baril, D.; Michot, C.; Armand, M. *Solid State Ionics* **1997**, *94*, 35–47.
- (19) Seki, S.; Susan, M. A. B. H.; Kaneko, T.; Tokuda, H.; Noda, A.; Watanabe, M. *J. Phys. Chem. B* **2005**, *109*, 3886–3829.
- (20) Minier, M.; Berthier, C.; Gorecki, W. *J. Phys. (Paris)* **1984**, *45*, 739–744.
- (21) According to the lot specification of the supplier, the PEO material used for the preparation of the present polymer electrolytes contained 1.6 wt % SiO<sub>2</sub>, 0.1 wt % CaO, and 200–500 ppm BHT as inhibitor.
- (22) Fauteux, D.; Lupien, M. D.; Robitaille, C. D. *J. Electrochem. Soc.* **1987**, *134*, 2761–2766.
- (23) Gorecki, W.; Jeannin, M.; Belorizky, E.; Roux, C.; Armand, M. *J. Phys.: Condens. Matter* **1995**, *7*, 6823–6832.
- (24) Bastek, J.; Stolwijk, N. A.; Köster, Th. K.-J.; van Wüllen, L. *Electrochim. Acta* **2010**, *55*, 1289.
- (25) Heddier, C. Diploma Thesis, University of Münster, 2012.
- (26) Fauteux, D.; McCabe, P. *Polym. Adv. Technol.* **1995**, *6*, 83–90.
- (27) Dreezen, G.; Ivanov, D. A.; Nysten, B.; Groeninckx, G. *Polymer* **2000**, *41*, 1395–1407.
- (28) Przylusky, J.; Wiczorek, J. *Therm. Anal.* **1992**, *38*, 2229–2238.
- (29) Muszynska, M.; Wycislik, H.; Siekierski, M. *Solid State Ionics* **2002**, *147*, 281–287.
- (30) Perrier, M.; Besner, S.; Paquette, C.; Vallée, A.; Lascaud, S.; Prud'homme, J. *Electrochim. Acta* **1995**, *40*, 2123–2129.
- (31) Minier, M.; Berthier, C.; Gorecki, W. *Solid State Ionics* **1983**, *9* & *10*, 1125–1128.
- (32) Bailey, F. E. Jr.; Koleske, J. V., *Poly(ethylene oxide)*; Academic Press: San Diego, CA, 1976.
- (33) Vallee, A.; Besner, S.; Prud'homme, J. *Electrochim. Acta* **1992**, *37*, 1579–1583.
- (34) Besner, S.; Prud'homme, J. *Macromolecules* **1989**, *22*, 3029–3037.

- (35) Robitaille, C.; Marques, S.; Boils, D.; Prud'homme, J. *Macromolecules* **1987**, *20*, 3023–3034.
- (36) Besner, S.; Vallee, A.; Bouchard, G.; Prud'homme, J. *Macromolecules* **1992**, *25*, 6480–6488.
- (37) Kim, J. H.; Hong, S. U.; Won, J.; Kang, Y. S. *Macromolecules* **2000**, *33*, 3161–3165.
- (38) DiMarzio, E. A.; Gibbs, J. H. *J. Polym. Sci.* **1963**, *A1*, 1417.
- (39) Flory, P. J. In *Principles of Polymer Chemistry*; Cornell University Press: Ithaca, NY, 1953; p 495.
- (40) Reimschuessel, H. K. *J. Polym. Sci.* **1979**, *17*, 2447–2457.
- (41) Reich, S.; Michaeli, I. *J. Polym. Sci.* **1975**, *13*, 9–18.
- (42) Pradhan, D. K.; Choudhary, R. N. P.; Samantaray, B. K.; Katiyar, R. S. *Int. J. Electrochem. Sci.* **2007**, *2*, 861–871.
- (43) Ibrahim, S.; Johan, M. R. *Int. J. Electrochem. Sci.* **2012**, *7*, 2596–2615.
- (44) Suarez, S.; Abbrent, S.; Greenbaum, S. G.; Shin, J. H.; Passerini, S. *Solid State Ionics* **2004**, *166*, 407.
- (45) van Krevelen, D. W.; *Properties of Polymers*; Elsevier: Amsterdam, 2000.
- (46) Wu, W. B.; Chiu, W. Y.; Liao, W. B. *J. Appl. Polym. Sci.* **1997**, *64*, 411–421.
- (47) Suthanthiraraj, S. A.; Vadivel, M. K. *Ionics* **2012**, *18*, 385–394.
- (48) Dey, A.; Karan, S.; De, S. K. *Indian J. Pure Appl. Phys.* **2013**, *51*, 281–288.
- (49) Shin, J. H.; Passerini, S. *J. Electrochem. Soc.* **2004**, *151*, A238–A245.
- (50) Stolwijk, N. A.; Wiencierz, M.; Fögeling, J.; Bastek, J.; Obeidi, Sh. *Z. Phys. Chem.* **2010**, *224*, 1707–1733.
- (51) Fox, T. G.; Flory, P. J. *J. Appl. Phys.* **1950**, *21*, 581–591.
- (52) Beevers, R. B.; White, E. F. T. *Trans. Faraday Soc.* **1960**, *56*, 744–752.
- (53) Kelly, I. E.; Owen, J. R.; Steele, B. C. H. *J. Power Sources* **1985**, *14*, 13–21.
- (54) Lee, Y. L.; Christ, B. *J. Appl. Phys.* **1986**, *60*, 2683–2689.
- (55) The investigated P(EO–PO)<sub>30</sub>PMImI electrolyte is based on a random copolymer with the molar ratio PO/EO = 18/82 complexed with the ionic liquid 1-propyl-3-methylimidazolium iodide; see: Gaertner, D. Bachelor Thesis, University of Münster, **2012**.
- (56) Lauenstein, A.; Johansson, A.; Tegenfeldt, J. *J. Electrochem. Soc.* **1994**, *141*, 1819–1823.